

Mechanism of Cobalt Cluster Size Control in Co-MCM-41 during Single-Wall Carbon Nanotubes Synthesis by CO Disproportionation

Dragos Ciuparu,* Yuan Chen, Sangyun Lim, Yanhui Yang, Gary L. Haller, and Lisa Pfefferle

Department of Chemical Engineering, Yale University, New Haven, Connecticut 06520

Received: May 5, 2004; In Final Form: July 26, 2004

The mechanisms controlling the reduction of cobalt and the growth of metallic cobalt clusters in Co-MCM-41 catalysts at different stages in the process of single-wall carbon nanotubes (SWNT) synthesis were investigated both by in-situ and ex-situ X-ray absorption spectroscopy. We have found that prereduction of the catalyst in hydrogen at temperatures below 700 °C does not reduce the cobalt ions to metallic cobalt, but removes hydroxyl groups and oxygen ions creating oxygen vacancies and/or a partially reduced cobalt species. The prereduction treatment, however, does increase the density of electrons at the Fermi level weakening the interaction of Co^{2+} with the silica framework. Subsequent exposure of the catalyst to CO at 750 °C causes CO to strongly interact with the cobalt clusters most likely by the transfer of electrons into the d orbitals of Co. This strong interaction makes the cobalt more mobile at the surface and allows it to nucleate into clusters capable of dissociating CO and initiating the growth of SWNT. Prior to exposure to CO, the reduced cobalt species strongly interacting with the silica framework do not nucleate into larger clusters in the presence of He or H_2 , preserving near atomic cobalt dispersion, as determined by EXAFS.

Introduction

Because the electronic properties of the single-wall carbon nanotubes (SWNT) depend on their diameter and chirality,¹ their use in large scale production of electronic devices is hindered by the high purity and diameter uniformity of the SWNT required for such applications. Several processes^{2–4} synthesize SWNT of relatively high purity, among which the HiPCO and CoMoCAT processes are widely known. The CoMoCAT process was shown to produce SWNT with a narrow distribution of tube diameters with high selectivity.⁵

We have recently reported on our preliminary results moving toward the goal of being able to controllably preselect the diameter of the SWNT grown on a Co-MCM-41 catalyst.⁶ We observed that the diameter of the SWNT produced correlates with the size of the cobalt clusters formed in our catalyst during the SWNT synthesis process and that by controlling process conditions and catalyst design, we can control the metal cluster size/state.⁷ We have also observed a strong influence of the size of the cobalt clusters on their selectivity for SWNT and concluded that large cobalt particles are selective for amorphous carbon and graphite,⁸ in agreement with results reported by other groups.⁵ No metal particles were ever observed on the ends of the SWNT grown on Co-MCM-41 catalysts.

The good selectivity of the CoMoCAT process has been attributed to the presence of the molybdenum component in the catalyst, which stabilizes the oxidized cobalt against reduction and allows formation of small Co particles highly selective for production of SWNT.⁹ The mechanism behind this stabilization effect has been proposed to derive from the formation of a very stable surface Co molybdate-like structure, which is slowly disrupted in the presence of CO by the formation of Mo carbide. The released cobalt agglomerates into small clusters that subsequently initiate the growth of SWNT.¹⁰

In our Co-MCM-41 catalyst, the oxidized cobalt species were also observed to be stabilized against reduction under severe reducing conditions.⁷ We have proposed that the final size/state of the cobalt cluster and, thus, the uniformity of the diameter of the SWNT produced are most likely controlled by the relative rates of the several physical and chemical processes affecting the structure and the state of the catalyst during the SWNT synthesis: cobalt reduction and migration through the pore wall to the pore wall surface, cobalt nucleation and growth into clusters, and carbon deposition.¹¹ The experiments reported here were designed to investigate the mechanisms controlling the rates of cobalt reduction and cluster nucleation at different stages of the SWNT synthesis process.

Experimental Section

A Co-MCM-41 catalyst with 1 wt % cobalt loading (as determined by ICP-MS at Galbraith Laboratories, Knoxville, TN) was synthesized using a C16 organic template and a high purity Cab-O-Sil fumed silica source from Cabot Corporation. Because we have found the pH to strongly affect the reducibility of cobalt in the silica framework,¹² the pH was carefully controlled at 11.5 during the initial stage of the synthesis. Although this is likely near optimal for synthesizing Co-MCM-41 for carbon nanotube growth using the C16 alkyl template, SWNT growth as a function of pH during catalyst synthesis has not yet been optimized and likely varies with the alkyl chain length used as templating agent. The catalyst resulting from removal of the organic template by calcination had an average pore diameter of 28.5 ± 1 Å as determined from the nitrogen physisorption measurement using the BJH method.¹³ The nitrogen adsorption–desorption isotherms were measured at -196 °C with a static volumetric instrument Autosorb-1C (Quantachrome).

The state of the cobalt catalyst and the size of the cobalt clusters were determined from the X-ray absorption spectra

* To whom correspondence should be addressed.

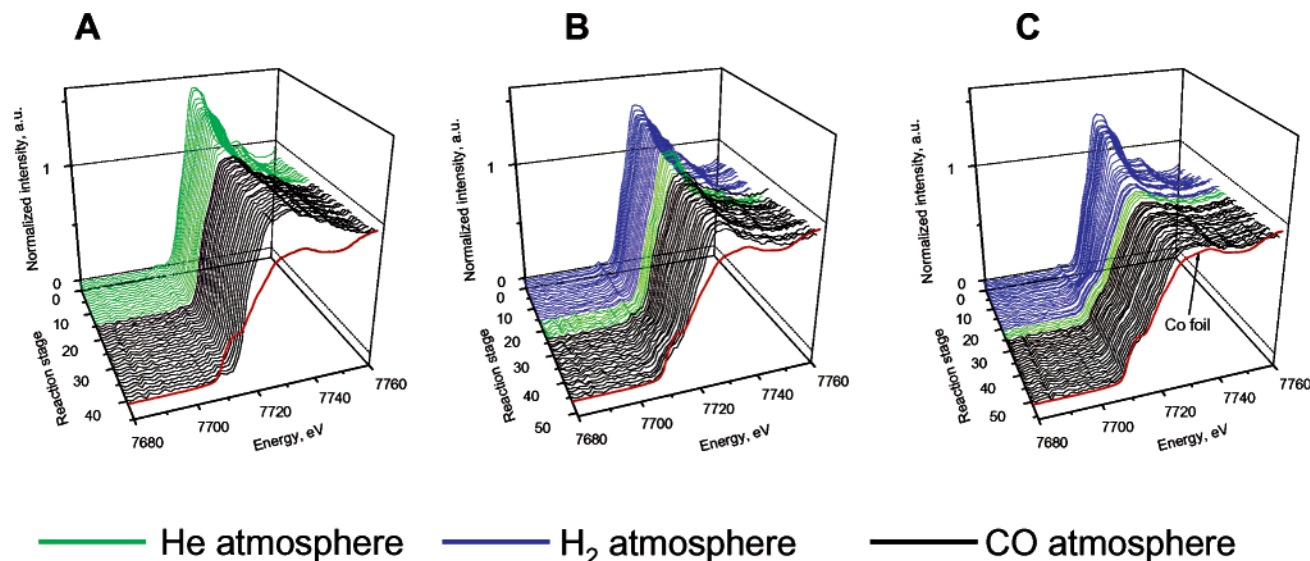


Figure 1. The XANES spectra recorded during Co-MCM-41 pretreatment under different conditions and SWNT synthesis at 750 °C for 1 h under 6 atm CO pressure: (A) no catalyst prereduction; (B) catalyst heating and prereduction in hydrogen at 500 °C for 30 min; (C) catalyst heating and prereduction in hydrogen at 700 °C for 30 min.

collected at beam line X23A2, National Synchrotron Light Source, Brookhaven National Laboratory. Two types of samples were measured: (i) ex-situ samples, consisting of catalysts submitted to different treatments and subsequently exposed to the ambient atmosphere, and (ii) in-situ samples, quenched at different stages of the carbon nanotube synthesis process and characterized before exposure to the ambient atmosphere. In-situ carbon nanotube growth experiments were performed to monitor the state of the catalyst during the SWNT synthesis process, consisting of the catalyst prereduction in hydrogen, heating in helium to the reaction temperature, and SWNT growth at CO pressures of 6 or 2 atm. For the in-situ experiments, 80 mg of fresh Co-MCM-41 were pressed at ~ 5 tons into a round self-supporting wafer (1.5 cm in diameter) using a hydraulic pellet press. The wafer was placed in the in-situ stainless steel reaction chamber described elsewhere.⁸ During the in-situ experiment, the sample was heated in flowing hydrogen from room temperature to 500 °C (or 700 °C) at 20 °C/min and reduced isothermally for 30 min. Then, the catalyst was purged with ultrahigh purity helium at 500 °C (or 700 °C) and then heated to 750 °C at 20 °C/min in flowing helium. For the in-situ assessment of the state of the catalyst during different reaction conditions, X-ray absorption near-edge structure (XANES) spectra were continuously collected from 30 eV below to 50 eV above Co K edge in 1 eV steps, averaging approximately 3 min per scan.

Analysis of the spectra collected for the ex-situ samples followed the procedures described in detail in our previous work.⁸ The EXAFS spectra recorded for ex-situ samples were calibrated to the edge energy of the cobalt foil internal reference. The background removal and edge-step normalization were performed using the FEFFIT code.¹⁴ The theoretical EXAFS functions for different cobalt species (Co, Co₃O₄) generated by the FEFF6 program¹⁵ were used to fit the experimental data to obtain the corresponding Co–Co and Co–O first-shell coordination numbers. Because of the short energy range of the in-situ XANES spectra, the postedge background of the XANES spectra was not long enough to obtain an accurate edge energy jump at E_0 . To compare the XANES features observed in different experiments, assuming a constant Co atom concentration under the X-ray beam during reaction, we used the energy edge intensity measured from the EXAFS spectrum of the same

sample recorded after each in-situ reaction XANES series. The normalized XANES spectra for each series of in-situ experiments were obtained by subtracting the smooth preedge absorption and the fixed edge step determined from the analysis of the final EXAFS spectrum, as described above.

Results and Discussion

A first series of in-situ XANES experiments was performed varying the catalyst pretreatment conditions but maintaining reaction conditions. For the first experiment, the catalyst was simply heated to 750 °C under flowing helium and then reacted for 1 h under 6 atm of CO pressure at 750 °C. For the next two experiments, the catalyst was heated in hydrogen to 500 °C or 700 °C, held at this temperature for 30 min, then purged with helium and heated in flowing helium to 750 °C prior to exposure to 6 atm CO for 1 h at 750 °C. The normalized XANES spectra collected during these treatments are given in Figure 1. The spectra in Figure 1 are gray density coded so that those recorded under flowing helium have a light gray hue, while those recorded while catalysts are reduced in hydrogen at the early stage of the experiment (reaction stage values below 15 and 20 in Figures 1B and 1C, respectively) or during exposure to CO at 750 °C (reaction stage values higher than 24 in Figures 1B and 1C) are plotted in dark gray hue. The spectrum of the cobalt foil is given in each plot for reference.

A few spectra from Figure 1B are plotted in Figure 2 without any offset to clearly observe the changes in the main spectral features. The insert of Figure 2 shows the derivative of the Co foil spectrum. Three regions of the XANES spectrum provide information concerning the state of the catalyst. The first region of interest in the XANES spectrum is the preedge peak, which was assigned to the dipole forbidden $1s \rightarrow 3d$ transitions whose intensities are strong functions of the local symmetry of the Co species.¹⁶ The second region of interest is the energy of the Co K edge, as defined by the second peak in the derivative of the EXAFS spectrum given in the inset of Figure 2. The position of the K edge varies linearly with the valence of the Co species. The K edge of the fully reduced Co shifts to lower energy compared to the edge of the fully oxidized Co. Unlike vanadium, however, whose reduction from V^{5+} to V^0 produces a relatively large shift in the energy of the K edge,¹⁷ Co exhibits a narrower

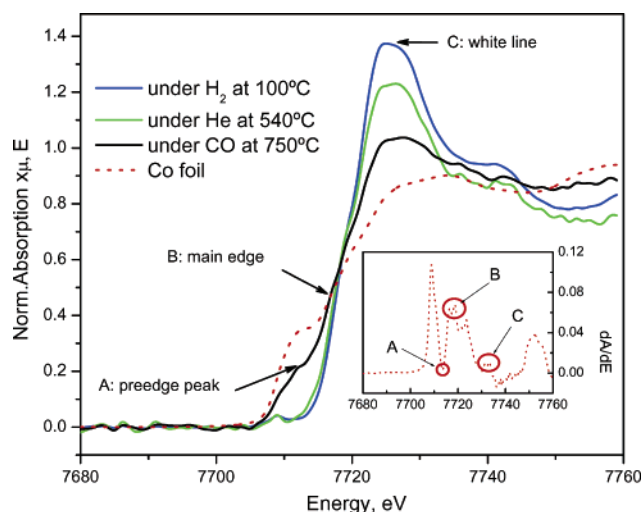


Figure 2. The XANES region of the EXAFS spectra recorded for Co-MCM-41 under different atmospheres and for the cobalt foil reference. The inset shows the energy values corresponding to the pre-edge peak (A), main edge energy (B), and white line (C) as determined from the first derivative of the EXAFS spectrum recorded for the Co foil. The maximum intensity of the white line (~ 7725 eV) observed with the Co-MCM-41 samples is shifted to lower energy compared to that observed for the Co foil (~ 7730 eV).

range of oxidation states (0 to +3) and our starting material, Co-MCM-41, has Co^{2+} isomorphously substituted for silicon ions.⁷ In our experiment, the K edge does not show significant shifts, in contrast with the other two spectral features. The intensity of the white line is the third region of interest since it is a direct measure of the density of empty states at the Fermi level of the cobalt species, with oxidized cobalt having a strong white line intensity, while the fully reduced Co metal produces a very weak white line feature.

The intensities of the pre-edge peak and of the white line were therefore selected as the two main features to monitor the

changes of the Co-MCM-41 catalyst during in-situ reaction. The normalized absorption intensity determined in the XANES spectra at the energy corresponding to the first minimum in the derivative of the Co foil spectra depicted by A in the inset of Figure 2 (i.e., 7713 eV) was considered the pre-edge peak intensity. The intensities of the white line peaks were determined similarly from the position of the second minimum depicted by C in the inset of Figure 2 (i.e., 7725 eV). The changes in the intensities of these spectral features determined for the experiments depicted in Figure 1 are given in Figure 3. The intensity of the white line was observed to decrease continuously as the samples were heated from room temperature to 500 °C in either flowing He or hydrogen (Figure 1A and 1B and Figure 3A and 3B). The initial decrease in the white line was not associated with any visible changes in the pre-edge feature of the spectra. These results indicate that during heating in hydrogen or helium the density of the electrons at the Fermi level of the oxidized cobalt increases. This is likely due to the surface dehydroxylation associated with formation of oxygen vacancies trapping one or two electrons each. Dehydroxylation, however, does not change significantly the symmetry of the cobalt ions since the pre-edge feature does not change. This implies that the hydroxyls removed from the surface are bound to silicon ions; thus, most of the cobalt ions are likely located inside the pore wall rather than exposed to the surface. Moreover, if the hydroxyls were bound to cobalt ions, their removal should have increased the oxidation state of the cobalt, which should have resulted in an increase in the white line intensity. Assuming an oxygen-terminated pore wall surface, as proposed by Feuston,¹⁸ and an oxygen ionic radius of 1.24 Å and 0.72 Å for Co^{2+} , since the pore wall thickness determined from X-ray diffraction data is approximately 10 Å,⁷ the minimum and the maximum depths in the pore wall at which a Co^{2+} ion can be found are approximately 2 and 4.3 Å, respectively. If the cobalt ions were located close to the surface, removal of their neighboring oxygen should affect both the white

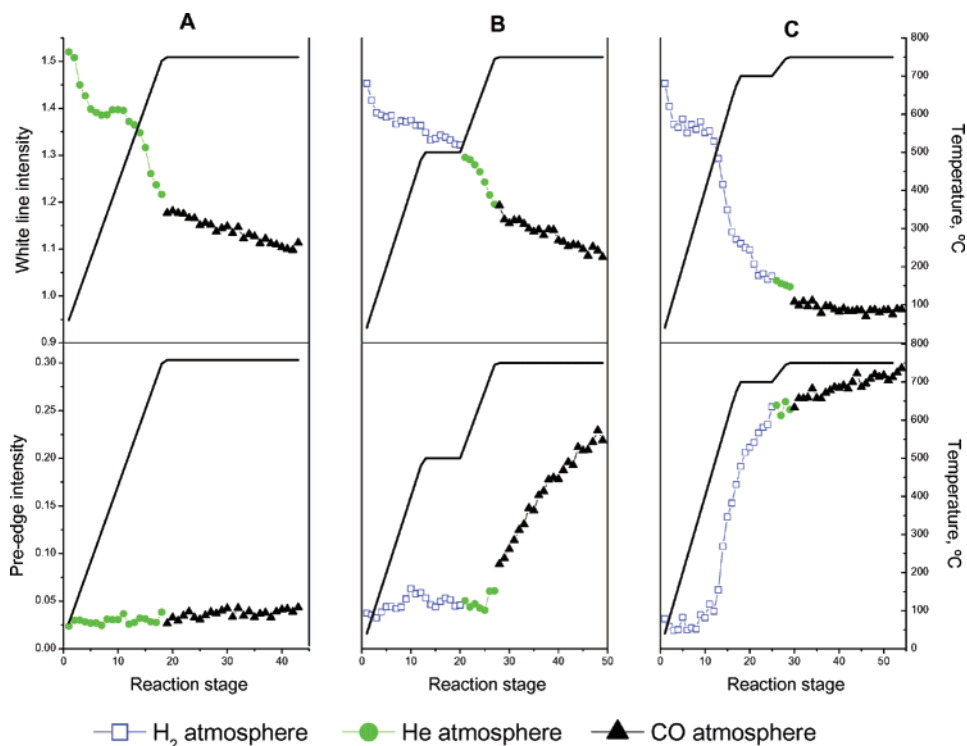


Figure 3. Variation of the intensities of the pre-edge feature and of the white line during different treatments. The scales are the same for both temperature (right side) and intensity (left side) for the two spectral feature series. The solid lines show the temperature profile corresponding to each experiment. Graphs A, B, and C were built using the XANES spectra in Figure 1A, 1B, and 1C, respectively.

line intensity and the preedge peak by changing both its oxidation state and symmetry. Along these lines, the cobalt ions are most likely located deeper in the pore wall. However, if the oxygen ion is replaced by an oxygen vacancy trapping two electrons, the preedge should not change, while the intensity of the white line can change significantly.

When the catalyst was heated in hydrogen to 700 °C (Figure 1C), a further decrease in the intensity of the white line was associated with a significant change of the preedge feature. The narrow and weak peak observed initially with the fully oxidized Co-MCM-41 samples at about 7709 eV becomes wider and more intense and shifts to 7713 eV, suggesting both a major change in the symmetry of the cobalt species and a broader distribution of the energy levels of the d orbitals that can accommodate the photoexcited core electron. These changes are most likely indicative of the formation of fully reduced, metallic cobalt clusters. In contrast, the catalyst heated in flowing helium after the pretreatment in hydrogen between room temperature and 500 °C with 30 min isothermal hydrogen reduction at 500 °C (Figure 1B) did not show any modification of the XANES spectra in the preedge region although the white line intensity continuously decreased. The cobalt could not be completely reduced when exposed to pure CO for 1 h even at 750 °C if the catalyst was not prerduced in hydrogen prior to the CO treatment (Figure 1A). In contrast, exposure to CO at 750 °C after prerduction with hydrogen at 500 °C does produce modifications of the preedge peak (Figure 1B). This behavior suggests that hydrogen prerduction at 500 °C produces changes in the electron density at the Fermi level of cobalt most likely due to the change of one or more of its ligands, or the $\equiv\text{Si}-\text{O}$ coordinated to Co (i.e., exchange of a OH ligand with an oxygen ion or an oxygen vacancy, either directly in the coordination sphere of Co, or of the Si bonded through oxygen to Co), or to the partial reduction to an intermediary state (i.e., Co^{+x}), but higher temperatures and the presence of a reducing atmosphere (CO or hydrogen) are required for the complete reduction of cobalt to metal (Co^0). The main question arising from these experiments is how are the two reduction processes, by CO and by hydrogen, different. At high enough temperatures, treatment in hydrogen can completely reduce the cobalt; however, reduction of the Co by CO requires pretreatment of the catalyst in hydrogen at 500 °C.

It is postulated that hydrogen can penetrate the silica pore wall and, by removal of surface oxygen from silica, causes formation and migration of oxygen vacancies that allow cobalt to become mobile in the silica. Thus, prerduction of the catalyst facilitates the access of the CO to the partially reduced cobalt species embedded in the MCM-41 pore wall. After prerduction in hydrogen at 500 °C, the reduced cobalt is still atomically dispersed and chemically interacting with the silica. No change in preedge peak is evidenced, consistent with cobalt preserving its local symmetry in tetrahedral coordination.

To characterize the degree of reduction at different stages in the process, samples quenched at different stages were investigated by EXAFS. The spectra recorded for samples quenched after prerduction at 500 and 700 °C for 30 min are plotted in R space in Figure 4 along with the spectrum recorded for a sample prerduced 30 min at 700 °C, heated in He to 750 °C, and exposed for 1 h to 6 atm CO at 750 °C. The major peaks centered at R values of approximately 1.6 and 2.2 Å correspond to the Co–O and Co–Co interactions, respectively. The spectrum for the sample prerduced at 500 °C shows an insignificant Co–Co peak suggesting a very small fraction, if any, of the cobalt ions in the silica framework has been

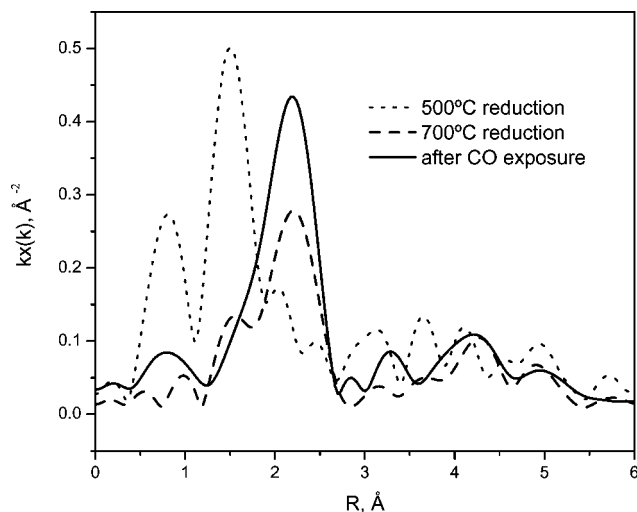


Figure 4. The EXAFS spectra plotted in R space for Co-MCM-41 samples exposed to different reducing treatments.

completely reduced to metal and made mobile to nucleate into small clusters to produce a Co–Co peak in the R space EXAFS spectrum. It is possible that there is some fully reduced cobalt after prerduction at 500 °C, but because these atoms remain isolated from other cobalt atoms in the silica framework they do not produce a Co–Co peak or a significant metallic preedge peak.

Prerduction at 700 °C, however, causes substantial Co reduction to the metal and nucleation into large clusters showing a strong Co–Co interaction in the EXAFS spectrum in Figure 4, as well as a significant metallic preedge peak (see Figure 3C). Despite the large fraction of reduced cobalt and, thus, the relatively high concentration of cobalt at the surface, the Co–Co coordination number is 4.2 indicating the metallic Co clusters contain approximately 12 atoms each, assuming the (111)-truncated hemispherical cubic octahedron model that was shown to provide the best approximation for the relation between the average coordination number and the size of small nanoparticles.¹⁹ That such a Co cluster is stable in hydrogen at 700 °C is unprecedented; a possible mechanism for cobalt cluster stabilization consists of anchoring on cobalt ions stabilized in the oxidized state by the radius of curvature effects and was discussed in detail elsewhere.⁷ Further 1-h exposure of the sample prerduced at 700 °C to CO at 750 °C results in almost complete reduction and allows cobalt particles to grow until the Co–Co coordination number reaches 6.4 (corresponding to clusters of 24 atoms), indicating some growth of the metallic clusters formed after prerduction at 700 °C.

The next experiments were performed to test the hypothesis of partially reduced Co remaining in the silica lattice after prerduction in hydrogen. Our previous experiments demonstrated that Co-MCM-41 samples in which all or some fraction of the cobalt ions were completely reduced to metal were easily reoxidized simply by exposure to the ambient atmosphere. A mild rereduction treatment in hydrogen at 400 °C for 30 min restored the state of the cobalt clusters observed prior to reoxidation by exposure to the ambient atmosphere. Such reoxidation should not be possible if the reduced cobalt clusters were not exposed at the surface, that is, if they were embedded within the silica framework. Two fresh Co-MCM-41 samples were reduced for 30 min in flowing hydrogen at 650 and 700 °C, respectively. After these pretreatments, the samples were exposed to the ambient atmosphere for several days prior to the measurement of their EXAFS spectra. The samples were pressed into self-supported pellets weighting 80 mg and mounted

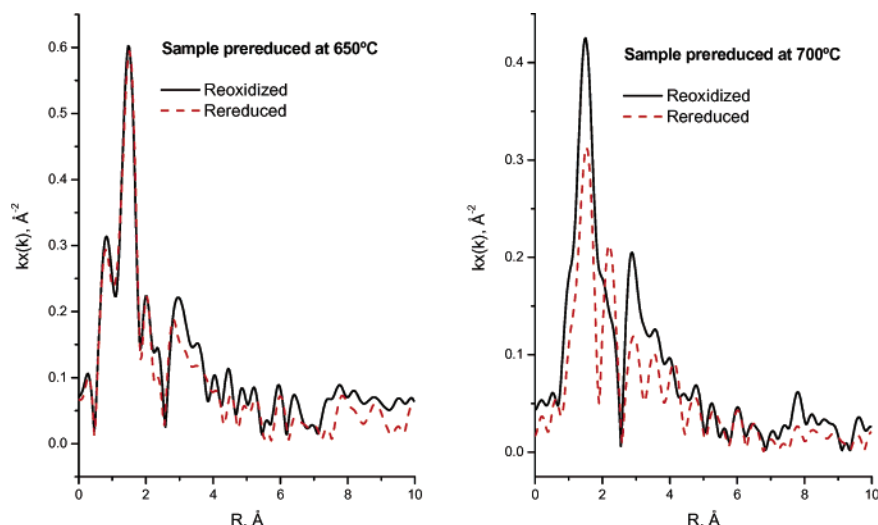


Figure 5. The EXAFS spectra in R space for samples prereduced at 650 and 700 °C after exposure to ambient air and mild rereduction in flowing hydrogen for 30 min at 400 °C.

in the in-situ X-ray absorption cell. The EXAFS spectra recorded both before and after the mild rereduction treatment at 400 °C described above are plotted in Figure 5. It becomes evident in the spectra in Figure 5 that the mild rereduction treatment does not produce visible modifications in the spectrum for the sample prereduced at 650 °C, but it dramatically changes the spectrum of the sample prereduced at 700 °C. A weak Co–Co peak is present in the sample prereduced at 650 °C. Since this reduction temperature is higher than the onset of reduction observed in a related TPR experiment using 5% H_2 in He ,⁷ this weak peak is likely associated with reduced cobalt species still embedded in the silica framework. After exposure to ambient oxygen, while the Co–Co peak is clearly visible in the sample prereduced at 650 °C, it appears only as a shoulder to the Co–O peak in the sample prereduced at 700 °C. However, after the mild rereduction treatment this shoulder becomes a well-defined, intense peak giving evidence for a strong Co–Co interaction in metallic cobalt in the sample prereduced at 700 °C (as is seen in Figure 4 without exposure to ambient oxygen), indicating that reduction at high temperatures leads to the formation of Co clusters at the pore wall surface that can be easily reoxidized upon exposure to air. These differences clearly show that only slight differences in the prereduction conditions, that is, a 50 °C difference in the prereduction temperature, produce significant changes in the state of the catalyst, suggesting the formation of cobalt clusters has a rather high activation barrier.

Even more interesting is the fact that the Co–Co peak in the sample prereduced at 650 °C is not affected by the mild rereduction treatment, as opposed to the behavior of the sample prereduced at 700 °C, suggesting that the metallic species formed by prereduction at 650 °C are not exposed at the surface, or that they are resistant against oxidation upon exposure to the atmospheric oxygen pressure.

The presence of small metallic clusters embedded in or anchored to the silica framework would require either the diffusion of cobalt atoms through the silica framework to nucleate into small metallic Co clusters or diffusion of the reduced atoms through the pore wall to the pore wall surface, migration and nucleation on the surface, and then reincorporation or anchoring of the cluster into the pore wall. Assuming an atomic dispersion of the Co^{2+} ions in the silica framework, for 1% weight cobalt loading each Co^{2+} ion is surrounded by approximately 146 silicon ions and twice as many oxygen ions. This translates into a significant distance of at least 30 Å that

a reduced Co atom would have to travel until it would be able to meet a second atom to nucleate into a cluster. Along these lines, both of the scenarios discussed above seem unrealistic.

An alternative explanation is that the reduced Co atoms diffuse through the pore wall to the surface and nucleate into clusters of a few cobalt atoms that have a reduced chemical reactivity toward reoxidation during exposure to the ambient atmosphere. This high stability against reoxidation may be related to the inability of these clusters to dissociate oxygen, that is, such small clusters may not be capable of dissociating oxygen inherently, or dissociation may be inhibited by anchoring to cobalt ions bound to the silica matrix or, indeed, by direct Co–Si interaction at an oxide ion defect in silica. Once these clusters reach a critical size/morphology/electronic state, they start dissociating oxygen and become oxidized when contacted with the oxygen from the air.

In our previous reports on SWNT synthesis using CO disproportionation on Co-MCM-41 catalysts, we proposed that very small cobalt metal clusters that are not active for SWNT growth can likely be present at the surface and explained that their inability to initiate the growth of SWNT may be related to the low solubility of carbon into the small metallic Co clusters, or to their inability to dissociate CO.¹¹ The behavior of the Co-MCM-41 sample prereduced at 650 °C can be explained along the lines of our previously proposed hypothesis and is consistent with the near-zero Co–Co coordination number determined from the EXAFS spectrum for this sample.

The Co–Co coordination number determined from the EXAFS spectrum recorded after the mild rereduction of the Co-MCM-41 sample prereduced at 700 °C was 4.2 and increased to 6.4 for the sample further exposed to 6 atm CO at 750 °C for 1 h. The low Co–Co coordination number observed with the sample prereduced at 700 °C, along with the relatively large fraction of the reduced cobalt suggested by the EXAFS spectra plotted in the R space in Figure 5, suggests that the growth rate of the Co clusters is low in a hydrogen atmosphere even at 700 °C. Although this is expected because of the low cobalt loading (1 wt %) in this sample, the strong interaction between the small Co clusters and the curved pore wall of the MCM-41 host may also play an active role in anchoring the small clusters to the surface. The strength of this interaction is likely a function of the radius of curvature of the pore wall

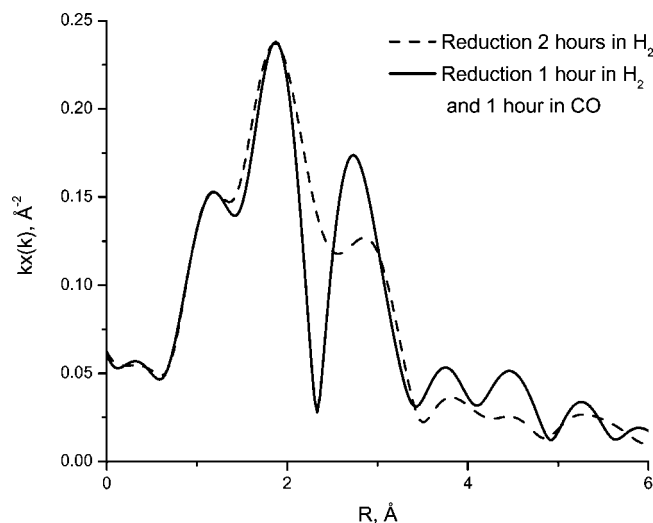


Figure 6. The EXAFS spectra in R space for Co-MCM-41 samples reduced 2 h in H_2 , or 1 h in H_2 , and 1 h in CO at atmospheric pressure and 650 °C.

offering an opportunity for “engineered” control, as discussed elsewhere.⁷

Assuming an oxygen-terminated pore wall surface as discussed above, a metallic cluster would be in contact with a layer of oxygen ions with a high density of electrons. Thus, a strong interaction between the Co cluster and this oxygen-terminated surface would imply a higher affinity for electrons for smaller Co metallic clusters. Such a strong interaction may be perturbed by adsorption of electron donor molecules, such as CO, leading to an increased mobility of the metallic cobalt clusters upon exposure to gas-phase molecules that can be bound at their surface. This is consistent with the sudden increase in the intensity of the preedge feature upon catalyst exposure to CO following prereduction in hydrogen for 30 min at 500 °C, as depicted in Figure 3B.

Indeed, the Co–Co coordination number observed for a Co-MCM-41 sample reduced in pure hydrogen at 650 °C for 2 h at atmospheric pressure was near zero, suggesting an atomic dispersion of the reduced cobalt in this sample. However, the EXAFS spectrum of this sample plotted in R space in Figure 6 shows a distinct Co–Co peak indicative of the presence of a few very small metallic clusters, confirming the complete reduction of some cobalt clusters observed for the sample reduced in hydrogen for 30 min at 650 °C (see Figure 5). When the same catalyst was reduced for 1 h in pure hydrogen and 1

h in pure CO at the same temperature and pressure, the Co–Co coordination number observed was 3.7 giving evidence for the formation of significantly larger cobalt clusters in the presence of CO compared to hydrogen. The intensities of the Co–O peaks for the samples exposed to different reduction strategies suggest that there is no significant difference in the degree of reduction for these two samples. Since we have shown that exposure of the Co-MCM-41 catalyst to 6 atm CO at 750 °C for 1 h only reduces the Co to a very small extent (see Figure 1A), these results are direct evidence that interaction of CO molecules with hydrogen prereduced Co-MCM-41 accelerates the growth of the Co clusters as discussed above and does not change significantly the rate of reduction. The same degree of reduction for the samples reduced for the same time either under hydrogen or both hydrogen and CO also suggests that the rate of metallic Co cluster formation is controlled by the diffusion of the cobalt species through the silica pore wall rather than by the reduction kinetics.

The intensities of the preedge peaks plotted in Figure 3 were obtained from the XANES spectra in Figure 1. In a hydrogen atmosphere, the metallic clusters interact more strongly with the surface because hydrogen is less likely to donate electrons to the Co cluster. Exposure to CO causes strong CO adsorption on the Co clusters weakening the interaction between the cluster and the pore wall surface, as discussed above. The clusters, thus, become more mobile at the surface and their nucleation rate increases until they reach the size/morphology/electronic state required to dissociate CO and initiate the growth of a carbon nanotube. Cobalt cluster growth ceases as the cobalt particles are covered with carbon, consistent with our previous findings that the Co–Co coordination number only increased during the first 30 min of exposure to CO.⁸

Along the lines of the scenario proposed above, the CO partial pressure should have a strong influence on the rate of cobalt nucleation on prereduced catalysts. Two XANES experiments were performed with Co-MCM-41 pretreated under identical conditions—heated to 500 °C and prereduced under flowing hydrogen for 30 min—and exposed to CO for 1 h at 2 and 6 atm, respectively. The XANES spectra recorded in situ during catalyst exposure to CO at 750 °C are shown in Figure 7. The variations of the intensities of the white line and of the preedge peak are plotted against the duration of the catalyst exposure to CO at 2 and 6 atm in Figure 8. Since the intensity of the preedge increases as the intensity of the white line decreases, it is likely that the variation of the intensity of the white line at these reaction conditions is reflective of the degree of cobalt

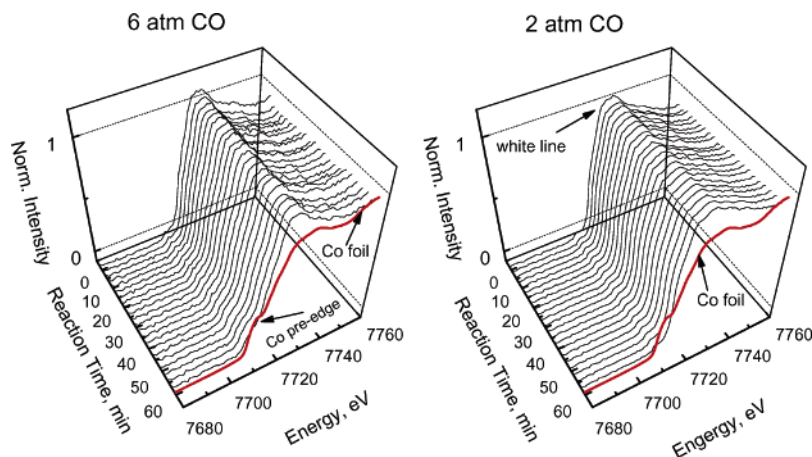


Figure 7. XANES spectra recorded during Co-MCM-41 exposure to CO at 750 °C and different pressures after identical pretreatment in hydrogen at 500 °C for 30 min.

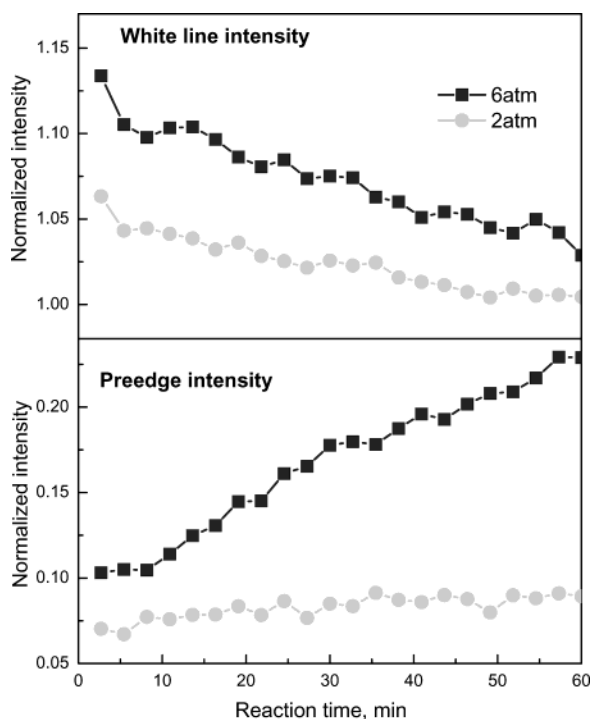


Figure 8. Variation of the intensities of the preedge peak and of the white line with the time of exposure to CO at 2 and 6 atm at 750 °C after identical pretreatments.

reduction to metal. The intensity of the white line decreased at approximately the same rate for the two pressures, suggesting the rate of cobalt reduction by CO is not highly sensitive to the CO pressure. The intensity of the preedge peak of the sample exposed 1 h to CO at 6 atm and 750 °C, however, increased at a significantly higher rate than that of the sample reacted for 1 h under 2 atm CO at the same temperature. Since both of the catalysts were exposed to identical pretreatment conditions, and the cobalt reduction rates suggested by the white line intensities are essentially identical, the concentration of the reduced cobalt species at the end of these experiments should be similar for the two samples. Therefore, the significant difference between the rates at which the intensity of the preedge peak increased suggests this spectral feature correlates rather with the size of the cobalt clusters, being an indication of the rate of cobalt nucleation and cluster growth. Indeed, the Co–Co coordination numbers determined for the samples pretreated under identical conditions and reacted with CO for 1 h at 750 °C at 2 and 6 atm were near zero and 4.6, respectively.

Since in a related X-ray diffraction investigation performed on Co-MCM-41 catalysts formation of cobalt silicate was observed only after calcination in oxygen at 900 °C, stabilization of cobalt in an oxidized silicate-like surface compound, similar to the cobalt molybdate-like surface layer in the Co–Mo catalysts, can be ruled out. The stabilization mechanism likely consists of the incorporation of the Co^{2+} ions in the silica rings forming the MCM-41 structure. The variation of the stability of these rings with ring size, as a function of radius of curvature of the pore wall, is discussed in detail elsewhere.⁷ This feature allows “engineering” of the Co cluster size and, potentially, of SWNT diameter.

Conclusion

The results presented here suggest that prereduction in hydrogen facilitates the removal of hydroxyl or oxygen from the Co-MCM-41. The oxygen vacancies created by hydrogen reduction allow Co to migrate to the surface and form small metal clusters strongly bound to the surface oxygen and exposed cations, but exposed to the gas phase. Bonding between these Co clusters and CO molecules weakens their interaction with the pore wall and increases their mobility allowing fast migration and formation of larger metallic clusters capable of dissociating CO and initiating the growth of SWNT. When the clusters become coated with carbon, however, their growth ceases. It could be that the minimum diameter of the SWNT that can be grown using a cobalt catalyst is limited by the size/morphology/electronic structure of the Co cluster required for dissociating the CO molecules to initiate the growth of the nanotube. A potential way to overcome this limitation may be the use of a different carbon precursor, such as alcohols or olefins. However, we are already near the ultimate limit, which is controlled by the ring strain as the SWNT diameter decreases.

Acknowledgment. We thank DARPA-DSO for the financial support for this project. Partial support for the synthesis of the Co-MCM-41 catalysts and the use of the National Synchrotron Light Source at Brookhaven National Laboratory was obtained from DoE-BES.

References and Notes

- (1) Ajayan, P. M.; Zhou, O. Z. *Carbon Nanotubes* **2001**, 80, 391.
- (2) Journet, C.; Maser, W. K.; Bernier, P.; Loiseau, A.; Lamy de la Chapelle, M.; Lefrant, S.; Deniard, P.; Lee, R.; Fischer, J. E. *Nature (London)* **1997**, 388, 756.
- (3) Nikolaev, P.; Bronikowski, M. J.; Bradley, R. K.; Rohmund, F.; Colbert, D. T.; Smith, K. A.; Smalley, R. E. *Chem. Phys. Lett.* **1999**, 313, 91.
- (4) Kitiyanan, B.; Alvarez, W. E.; Harwell, J. H.; Resasco, D. E. *Chem. Phys. Lett.* **2000**, 317, 497.
- (5) Resasco, D. E.; Alvarez, W. E.; Pompeo, F.; Balzano, L.; Herrera, J. E.; Kitiyanan, B.; Borgna, A. *J. Nanoparticle Res.* **2002**, 4, 131.
- (6) Ciuparu, D.; Chen, Y.; Lim, S.; Haller, G. L.; Pfefferle, L. *J. Phys. Chem. B* **2004**, 108, 503.
- (7) Lim, S.; Ciuparu, D.; Chen, Y.; Yang, Y.; Pfefferle, L.; Haller, G. L. *J. Phys. Chem. B* **2004**, ASAP DOI:10.1021/jp048881(+).
- (8) Chen, Y.; Ciuparu, D.; Lim, S.; Yang, Y.; Haller, G.; Pfefferle, L. *J. Catal.* **2004**, 225, 453.
- (9) Alvarez, W. E.; Kitiyanan, B.; Borgna, A.; Resasco, D. E. *Carbon* **2001**, 39, 547.
- (10) Herrera, J. E.; Balzano, L.; Borgna, A.; Alvarez, W. E.; Resasco, D. E. *J. Catal.* **2001**, 204, 129.
- (11) Chen, Y.; Ciuparu, D.; Lim, S.; Yang, Y.; Haller, G.; Pfefferle, L. *J. Catal.* **2004**, 226, 351.
- (12) Lim, S.; Yang, Y.; Ciuparu, D.; Wang, C.; Chen, Y.; Pfefferle, L.; Haller, G. *Top. Catal.* **2004**, in press.
- (13) Barrett, E. P.; Joyner, L. G.; Halenda, P. P. *J. Am. Chem. Soc.* **1951**, 73, 373.
- (14) Stern, E. A.; Newville, M.; Ravel, B.; Yacoby, Y.; Haskell, D. *Physica B* **1995**, 209, 117.
- (15) Ankudinov, A. L.; Ravel, B.; Rehr, J. J.; Conradson, S. D. *Phys. Rev. B* **1998**, 58, 7565.
- (16) Bart, J. C. J. *Adv. Catal.* **1986**, 34, 203.
- (17) Wong, J.; Lytle, F. W.; Messmer, R. P.; Maylotte, D. H. *Phys. Rev. B* **1984**, 30, 5596.
- (18) Feuston, B. P.; Higgins, J. B. *J. Phys. Chem.* **1994**, 98, 4459.
- (19) Frenkel, A. I.; Hills, C. W.; Nuzzo, R. G. *J. Phys. Chem. B* **2001**, 105, 12689.